HiSST: International Conference on
High-Speed Vehicle Science Technology
26–29 November 2018, Moscow, Russia

Development of a Mars Entry Condition at Flight Duplicated Enthalpy and Reynolds Number in the X2 Expansion Tube

Ranjini. Ramesh[1], Richard G. Morgan[2], Christopher M. James[3], David J. Mee[4]

Abstract

To support the development of thermal protection systems for future missions to Mars, obtaining turbulent heat transfer data using ground test facilities is crucial. This paper reports on the development of a high enthalpy, high Reynolds number turbulent flow condition for a representative Mars entry in the X2 expansion tube at the University of Queensland. The aim is to use the established flow condition to measure turbulent heat flux at Mars entry conditions using infrared thermography. A point in the trajectory of Mars Science Laboratory after transition to turbulence has been chosen for experimental investigation using the X2 expansion tube. The total enthalpy and post shock Reynolds number from experiments were tailored to match the corresponding flight values, addressing one of the key challenges in producing test conditions in a ground test facility to measure turbulent heating. The current study details the theoretical and experimental work that was undertaken to design and establish a test condition at flight duplicated enthalpy and post shock Reynolds number. It is expected that the work presented in this paper will provide a framework for designing and establishing test conditions that lie outside the typical operating range of X2 in the future.

Keywords: *Mars entry, ground testing, expansion tube, Reynolds number, flight duplicated enthalpy*

Nomenclature

BET – Best Estimated Trajectory
CEV – Crew Escape Vehicle
MSL – Mars Science Laboratory
p_1 – Shock tube fill pressure
p_5 – Acceleration tube fill pressure
ρ – Density
L – Characteristic Length Scale
TPS – Thermal Protection Systems

[1] *PhD Candidate, School of Mechanical and Mining Engineering, University of Queensland, r.ramesh@uq.edu.au*
[2] *Director at Center for Hypersonics, School of Mechanical and Mining Engineering, University of Queensland, r.morgan@uq.edu.au*
[3] *Post Doctoral Research Fellow, School of Mechanical and Mining Engineering, University of Queensland, c.james4@uq.edu.au*
[4] *Professor at Center for Hypersonics, School of Mechanical and Mining Engineering, University of Queensland, d.mee@uq.edu.au*

1. Introduction

Surface heating during planetary entry at hypersonic speeds has been a major challenge and concern for TPS designers since the early days of spaceflight [1]. Recently, the problem of turbulent heating has become a concern for vehicles such as Mars Science Laboratory (MSL) and Crew Escape Vehicle (CEV) [2]. In particular, for MSL the uncertainty in the aeroheating environment of the heatshield was more than 50% due to surface chemistry, early transition to turbulence and ablation induced roughness [3]. Higher uncertainties in transitional/turbulent heating rates lead to larger safety factors in the design of heat shields at the cost of reduced payload fractions and increased mass of the heat shield.

Further understanding of boundary layer transition and its effect on surface heating is required to decrease uncertainties and increase payload fractions associated with heat shield design. Several ground tests were conducted to obtain turbulent heat transfer data at high enthalpy Mars entry conditions [4-8]. Similarly, tests were conducted in HIEST at low enthalpy air conditions with roughness elements to measure heat transfer [9]. One of the major challenges encountered with these previous tests was the ability to generate turbulent flow at flight enthalpies on a blunt body. Hollis et al. [8] were able to trip the flow to turbulence at flight enthalpies on a sharp cone. However, this is not representative of a blunt planetary entry vehicle. Additionally, the majority of these tests have been conducted in an expansion tube due to the unique ability of an expansion tube to achieve high enthalpies and Reynolds numbers simultaneously.

It is important to decrease the uncertainties associated with designing and validating Mars entry vehicles for future Mars missions. Mars 2020, which is based on the MSL design, is expected to experience turbulent heating. With turbulent heating being a major driving factor for TPS design, it is important to obtain turbulent heat transfer data on the ground to continue the development of TPS for future missions. To do so, it is proposed to use X2 to measure turbulent heating in a high Reynolds number shock layer in a Martian atmosphere using infrared thermography. To facilitate such studies, a high Reynolds number test condition will need to be designed and established in the X2 expansion tube.

This paper discusses the design and establishment of a Mars entry condition at flight duplicated enthalpy and Reynolds number in X2. The condition to be designed is based on a turbulent point in the MSL trajectory. Furthermore, this work will also provide a framework for designing and establishing test conditions that lie outside the typical operating range of X2.

The X2 expansion tube at the University of Queensland is typically used to study high enthalpy planetary entry phenomena at speeds between 6 and 15 km/s. Studying Mars entry flows in an expansion tube involves lower speeds and higher static and stagnation pressures presenting a challenge which this study discusses.

2. X2 Expansion Tube Facility Description

The current experiments were performed in the X2 expansion tube at the University of Queensland. Fig 1 is a schematic of the X2 expansion tube with the x-t diagram also presented. The tunnel is instrumented with 14 PCB pressure transducers that are used to measure the shock speeds. The measured shock speeds are compared with the theoretical predictions to assess if the wave processes are being simulated accurately. X2 is a free piston driven expansion tube that is used to study planetary entry phenomena into atmospheres such as Earth [10], Venus [11] and Mars [12]. A more detailed overview of X2 can be found in Gildfind et al. [13].

All sections are evacuated before operation and then filled with the required gases. A scored steel plate acts as the primary diaphragm and an Aluminium foil secondary diaphragm separates the shock and acceleration tube.

The piston is held at the end of the cavity by vacuum. Operation begins when the piston is released. The high pressure air in the reservoir behind the piston compresses the driver gas until the primary diaphragm ruptures. This drives a shock through the test gas processing it until it reaches the secondary diaphragm. The shock then bursts the secondary diaphragm processing the test gas through an unsteady expansion into the acceleration tube, increasing the enthalpy of the flow.

The test gas then flows through the nozzle and enters the test section starting the test time. The test time is terminated by the arrival of the unsteady expansion of the downstream edge of the test gas or other wave processes. It is the unique operating principle of an unsteady expansion into the acceleration tube that allows expansion tubes to achieve high enthalpy and high Reynolds number flows simultaneously.

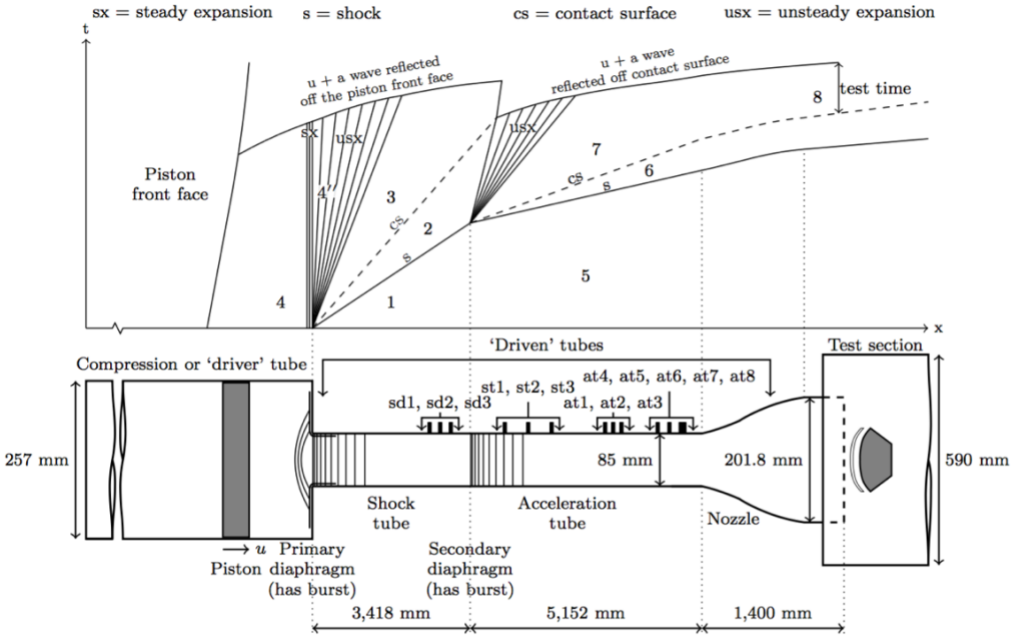

Fig 1. Schematic of X2 expansion tube and x-t diagram [13]

This facility currently utilises three steel primary diaphragms of varying thicknesses that can each be used with a driver gas of Helium or a mixture of Helium and Argon. These parameters are used with a range of fill pressures for the shock and acceleration tube to generate a wide range of freestream flow properties.

3. Flow Condition Development in X2

Achieving a desired test condition in an expansion tube requires the selection of appropriate input parameters that affect the resulting test flow. Additionally, direct measurement of flow properties are difficult due to the harsh experimental conditions. As explained by Gildfind et al [13], the test flow needs to be characterised in terms of the following parameters:

- Shock speeds
- Steady test time
- Core flow diameter
- Chemical/thermal composition of the test gas
- Static temperature, pressure and velocity

The procedure that was used to characterise each of the above parameters, using a combination of experimental and numerical work is detailed next.

The goal of designing the current condition is to generate a high Reynolds number turbulent boundary layer near the surface of a scaled vehicle in a Martian atmosphere. Given that the designed condition will be used to measure turbulent heat transfer, it is important to match total enthalpy and post shock Reynolds number as closely as possible. This is achieved by using binary scaling [14].

Binary scaling conserves the total enthalpy and ρL product between ground and flight [15]. The post shock Reynolds number is also conserved as a result of duplicating the post shock ρL product. Due to the Mach number independence principle [16], partial similarity to the flight post shock flow field can be achieved. It is important to match the post shock Reynolds number to obtain a similar boundary layer. Since the Mach number on the ground is lower than the flight Mach number, the total pressure loss across the shock will be lower on the ground. The post shock conditions can then be generated at lower total pressures than flight.

Since scaled testing was performed in X2, to maintain the flight ρL product with a decrease in the flight vehicle size, the density produced on the ground was much higher than the flight density. Since the core flow diameter in X2 is about 100 mm, a flight-to-ground scaling factor of 1:45 was used.

In the current study, condition design and establishment was performed in two steps. The first step was to generate a performance envelope for a chosen driver configuration to obtain an initial fill condition. The second step was to verify this experimentally to establish the final test condition. Each of these steps is discussed in further detail in sections 3.2 and 4 respectively.

3.1. Target Flow Conditions

Mars Science Laboratory was the first Mars entry vehicle to experience turbulent peak heating. Due to the large size and mass of MSL, preflight analysis and testing concluded that boundary layer transition would take place before peak heating [17, 18]. Post flight analysis showed this was the case and indicated the time in the Best Estimated Trajectory (BET) at which the flow became turbulent [19]. Hence a turbulent flow condition was chosen for condition design and establishment. The details of the trajectory point are listed in Table 1 and has been extracted from the BET.

Table 1. Details of chosen MSL trajectory point [19]

Parameter	Value
Altitude (km)	36.6
Velocity (m/s)	5584
Mach Number	25
Freestream Reynolds Number	2.31×10^6
Post shock Reynolds Number	1.68×10^5
Total Enthalpy (MJ/kg)	15.6

Note that the total flow enthalpy at this point on the trajectory is calculated using only the velocity component of the total enthalpy as the true flight condition has a low free-stream temperature making the static enthalpy negligible.

The simulation parameter is the post shock Reynolds number based on the equilibrium post shock conditions. The scaled post shock conditions to be achieved in the X2 expansion tube for a 100 mm diameter model are listed in Table 2.

Table 2. Target Flow Conditions

Parameter	Value
Total Enthalpy(MJ/kg)	15.6
ρL product (kg/m^2)	0.076
Post shock density (kg/m^3)	0.76
Post shock Reynolds Number	1.68 x 10^5

3.2. Theoretical Analysis

The performance envelope for the x2-lwp-2mm driver [20] was generated using PITOT [21]. PITOT is UQ's in-house expansion tube simulator which models the flow using compressible and isentropic flow relations. For a range of given inputs, PITOT calculates the pressure, temperature, density and velocity at each state in the expansion tube.

PITOT condition builder can generate a performance envelope by using the following inputs:

- Driver configuration – diaphragm thickness and driver gas
- Range of shock and acceleration tube fill pressures
- Test gas

All PITOT simulations were completed with X2's nozzle using a geometric area ratio of 5.64 and were run in fully theoretical mode. All test conditions discussed in this paper use a test gas composition of 96% CO_2, 4% N_2 for Mars entry. An initial operational envelope of the 2 mm driver indicated that the target flow conditions can be achieved with a 80% He, 20% Ar driver gas.

For the chosen driver configuration, a performance envelope was generated by varying the shock and acceleration tube fill pressures from 4 – 15 kPa and 450 – 1000 Pa respectively. The resulting change in total enthalpy, post shock density and post shock Reynolds number with these parameters are shown in Fig 2-3 with the target flow conditions also indicated. An initial operating condition which satisfied the target flow conditions was chosen using these performance envelopes and is listed in Table 3.

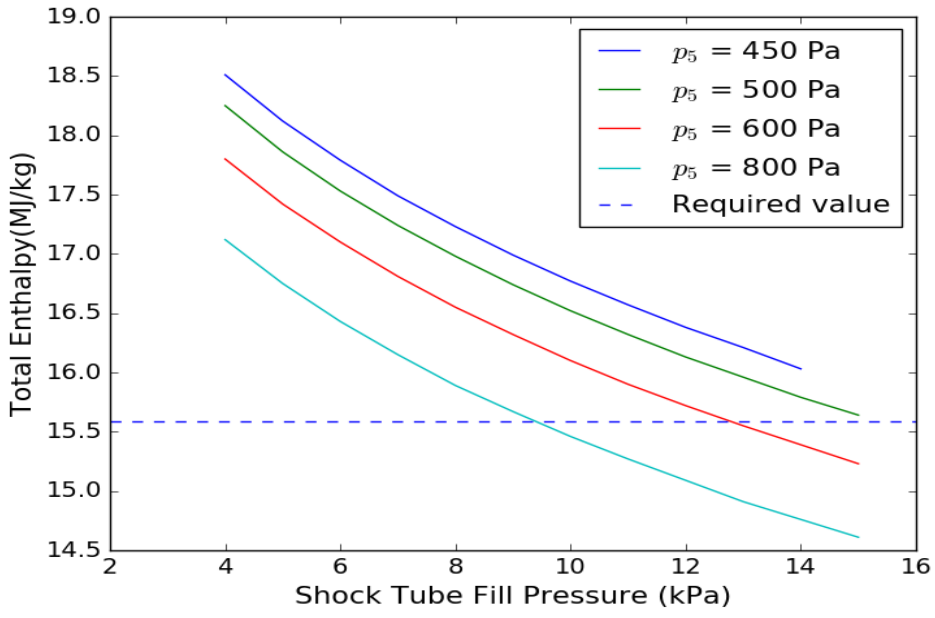

(a) Total enthalpy

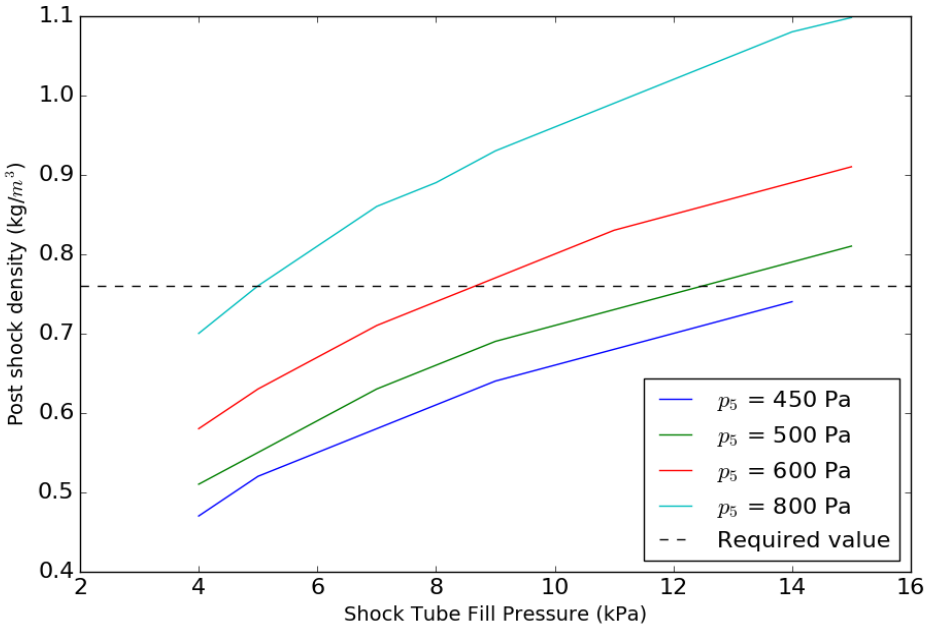

(b) Post shock density

Fig 2. Effect of varying p_1 and p_5 on (a) total enthalpy (b) post shock density for the 2 mm driver

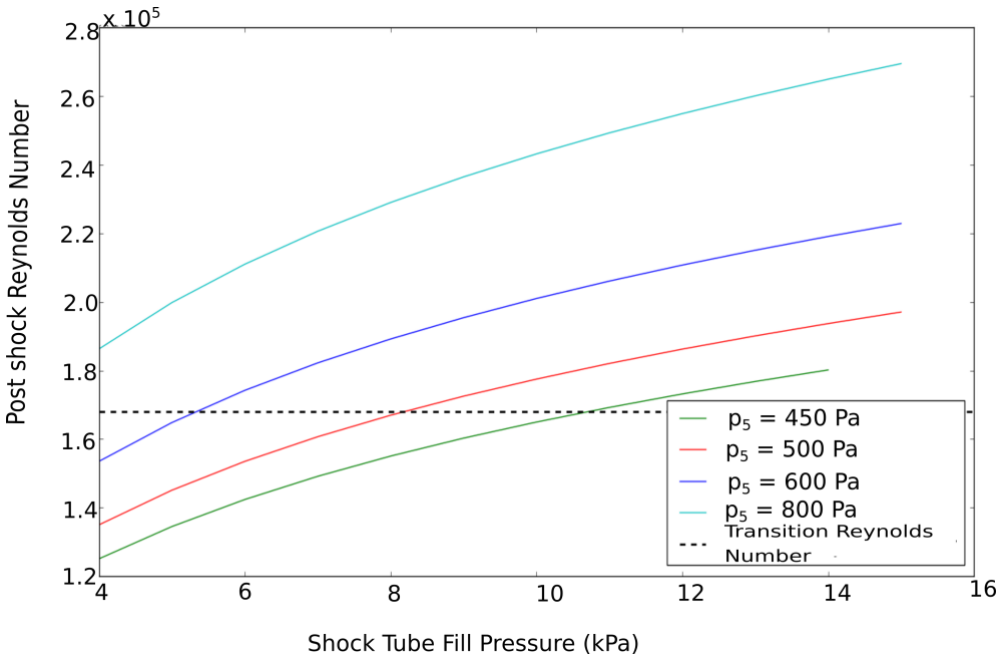

Fig 3. Effect of varying p_1 and p_5 on the post shock Reynolds number

Table 3. Initial operating condition

Driver	p_1(kPa)	p_5(Pa)	Test Gas(by Volume)	Driver Gas (by Volume)
X2-LWP-2 mm	13	500	96% CO_2, 4% N_2	80% He, 20% Ar

4. Experimental Analysis

4.1. Experimental Set-Up

To characterise the test flow, a nine probe pitot rake was mounted vertically in the test section and placed 5 mm axially from the nozzle exit. The centre probe 'pt5' was aligned with the centreline of the nozzle. Test section pressures were measured using 15° half angle coneheads [22] with a probe spacing of 17.5 mm.

Shock speeds were measured using the PCB pressure transducers in the shock and acceleration tubes as indicated in Fig. 1. All shock speeds presented hereafter were computed between sd1-sd3 for the shock tube and at4-at6 for the acceleration tube. A Shimadzu (HPV-1) high speed camera was used to record the test flow, luminosity before, during and after the experimental test time.

4.2. Experimental verification

Two shots were conducted at the operating condition identified in Table 3. The resulting experimentally measured properties are compared with PITOT predictions in Table 4.

There is a significant difference between the predicted and measured secondary shock speeds and conehead pressures. These differences can be attributed to the presence of viscous effects in the acceleration tube and nozzle [23, 24]. The boundary layer begins to grow at the start of the acceleration tube and then grows throughout the nozzle, thereby reducing the effective diameter of the tube and modifying the area ratio of the nozzle. PITOT can be modified to account for these effects.

Table 4. Mean experimental results compared with PITOT predictions

Parameters	Experimental	Theory
Primary shock velocity (m/s)	3401 ±24	3242
Secondary shock velocity (m/s)	5500 ±43	5166
15° conehead pressure (kPa)	92 ±28%	121

4.3. Fine-tuning the analytical model

The procedure that was used to fine-tune the PITOT model was as follows:

1. The velocity of the expanded test gas was set to flow behind the shock and the predicted pressure was compared with the experimental pressure.
    (a) If the predicted pressure was lower than the experimental value, then the setting was changed to shock-speed and the value of the expansion factor was reduced from one until the two results match. This accounts for viscous effects as noted by Mirels' [23]

    (a) If the predicted pressure was higher than the experimental value, no changes were made. This does not account for viscous effects.
2. The theoretical conehead pressures were compared with the experimental conehead pressures

(a) If the predicted conehead pressure was lower than the experimental value, then the area ratio was reduced from the geometric area of 5.64 until the predicted and experimental results match

(b) If the predicted conehead pressure was higher than the experimental value, then the area ratio was increased from the geometric area of 5.64 until the predicted and experimental results match

The correction factors applied are shown in Table 5. The refined model was then used to provide a new operating condition which is listed in Table 6.

Table 5. Correction factors in PITOT

Correction factors	
Expand test gas to	Shock speed
Expansion factor	0.895
Nozzle area ratio	9.0

Table 6. Final operating condition

Driver	**p_1(kPa)**	**p_5(Pa)**	**Test Gas(by Volume)**	**Driver Gas (by Volume)**
X2-LWP-2 mm	13	630	96% CO_2, 4% N_2	80% He, 20% Ar

4.4. Final test condition

Table 7 details the mean experimental data for four shots at the new operating condition. The shock speeds and the operating condition are input in PITOT's experimental mode to obtain the freestream and post shock properties as identified in Table 8.

Table 7. Mean measured properties of final test condition

Measured Quantities	
Primary shock velocity (m/s)	3372 ±24
Secondary shock velocity (m/s)	5349 ±41
15° cone pressure (kPa)	120 ±26%

Table 8. Detailed test flow properties for final test condition in X2

Parameter	**Value**
Total Enthalpy (MJ/kg)	15.7
Pitot Pressure (MPa)	1.24
Flight Equivalent Velocity (m/s)	5611
Freestream properties	
Mach Number	7.13

Reynolds Number	3.49 x 10^5
Velocity (m/s)	5045
Temperature (K)	2271
Pressure (kPa)	23.3
Post shock properties	
Density (kg/m^3)	0.75
Reynolds number	1.86 x 10^5
Temperature (K)	4790
Pressure (MPa)	1.2

Fig 4. shows the experimental 15° half angle conehead pressure traces for the tested condition. The results for shot x2s3800 are representative of all the conehead pressure traces seen for this condition. The data was filtered using a lowpass filter with a cut-off frequency of 100 kHz.

The first spike in the pressure trace corresponds to accelerator gas arrival. The accelerator gas is replaced by the arrival of the test gas and the nozzle start up process. The pressure remains steady for 140 μs which is the steady test time as shown in Fig 4. The pressure rise following this corresponds to the arrival of the driver gas.

The pressures for probes 'pt1' and 'pt9' are lower than those for the others probes indicating that they lie outside the core flow. Considering the geometry of the pitot rake, the core flow diameter was determined to be about 100 mm. The average conehead pressure ignoring the above listed probes for all experiments was 121 ± 3 kPa. This compares very well with a theoretical pressure of 118 kPa from PITOT.

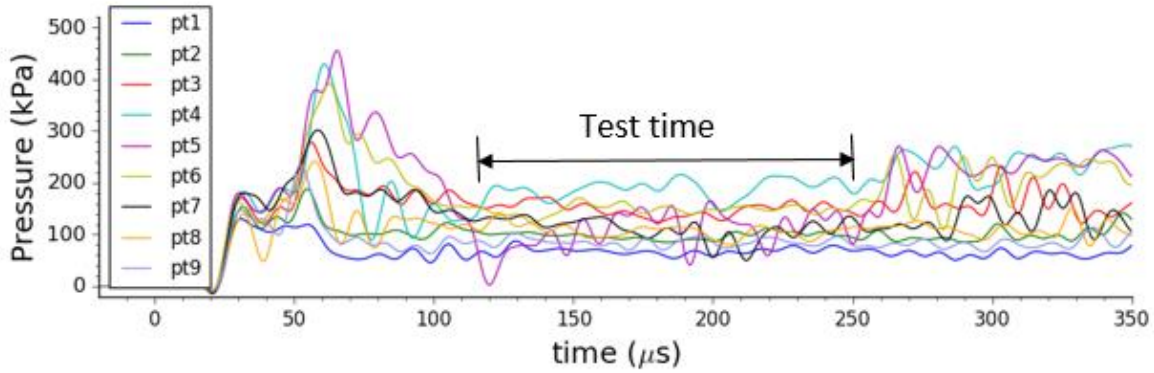

Fig 4. Experimental 15° half angle conehead pressure trace for x2s3800 with the steady test time indicated

The final detailed operating condition is shown in Table 9.

Table 9. Detailed operating condition for the 2mm driver

Reservoir fill condition	6.75 MPa Air
Driver fill condition	74.2 kPa Helium, 92.8 kPa Argon
Primary diaphragm	2 mm thick scored steel plate

Shock tube fill condition	13 kPa 96% CO_2, 4% N_2 (by volume)
Secondary diaphragm	1 x 18 μm thick Aluminium diaphragm
Acceleration tube fill condition	630 Pa air

4.5. Chemical Composition of the Test Flow

Fig. 5 shows the equilibrium mole fraction of the seven major species on a log scale for the designed condition as obtained in PITOT. Since the freestream temperature in X2 is greater than that in flight, the freestream flow in X2 is partially dissociated. Behind the shock, most of the CO_2 and N_2 has dissociated forming large concentrations of CO and O. It is important to note that at this speed for a Martian entry condition, the majority of shock layer species are molecular in nature with no ionised species present.

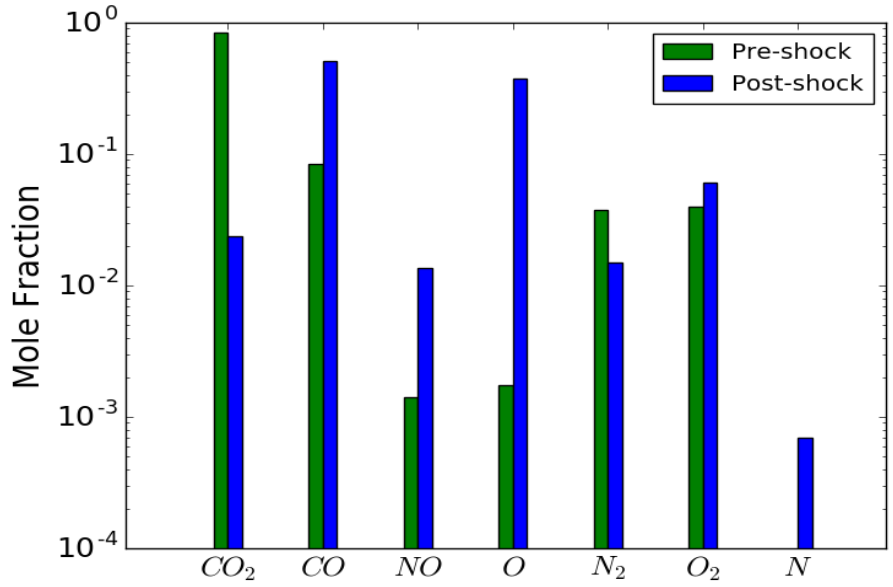

Fig 5. Concentration of freestream and post shock species for the designed condition

5. Comparison with target flow conditions

Table 10 compares the target flow condition with the actual test flow. It is important to note that when compared with the target flow conditions, the flight total enthalpy and post shock Reynolds number have both been duplicated.

Table 10. Comparison of final test condition with target flow conditions

Parameter	Target Flow Condition	Actual Value	Percentage Difference
Total Enthalpy(MJ/kg)	15.6	15.7	0.6
Post shock density (kg/m^3)	0.76	0.75	1.3
Post shock Reynolds number	1.68 x 10^5	1.86 x 10^5	10.7

6. Conclusion

A Mars entry condition at flight duplicated enthalpy and Reynolds number has been developed and experimentally verified in X2. The magnitude of the variation between individual shots were less than 2% for the shock speeds and less than 3% for the post shock density, total enthalpy and post shock Reynolds number. The test time was estimated to be 140 microseconds. The tools and techniques to design a condition in X2 were also discussed. The designed condition will be used to measure turbulent heat transfer using infrared thermography.

Acknowledgements

The authors would like to thank all the X2 operators for their assistance in operating the facility. This research is supported by the Australian Research Council (ARC) and an Australian Government Research Training Program (RTP) Scholarship.

References

1. Cohen, N., Jr. Eggers, A.: Progress and problems in atmospheric entry. NASA-tm-x-56885, Eng.Tech.Rep 1965
2. Hollis, B.: Blunt-Body Entry Vehicle Aerothermodynamics: Transition and Turbulence on the CEV and MSL Configurations. Paper presented at 40th Fluid Dynamics Conference and Exhibit, Chicago, 28 June – 1 July 2010
3. Gazarik, M., Wright, M.J., Little, A., Cheatwood, N.F., Herath, J.A., Munk, M.M., Novak, F.J.: Overview of the MEDLI project. Paper presented at the 2008 IEEEAerospace Conference, Big Sky, MT, USA, 1-8 March 2008
4. Hollis, B., Prabhu, D., Maclean, M., Durfrene, A.: Blunt Body Aerothermodynamic Database from High-Enthalpy Carbon-Dioxide Testing in an Expansion Tunnel. J. Thermophys. Heat. Transf. **31**, 712–731 (2017)
5. Hollis, B., Perkins, J.: High-Enthalpy Aerothermodynamics of a Mars Entry Vehicle Part 1: Experimental Results. J. Spacecr. Rockets. **34**, 49-456 (1997)
6. Wright, M., Olegjniczak, J., Brown, J., Hornung, H., Edquist, K.: Modeling of Shock Tunnel Aeroheating Data on the Mars Science Laboratory Aeroshell. J. Thermophys. Heat. Transf. **20**, 641–651 (2006)
7. MacLean, M., Dufrene, M., Carr, Z., Parker, R., Holden, M.: Measurements and Analysis of Mars Entry, Descent, and Landing Aerothermodynamics at Flight-Duplicated Enthalpies in LENS-XX Expansion Tunnel, Paper presented at AIAA SciTech Forum 53rd AIAA Aerospace Sciences Meeting, Florida, 5-9 January 2015
8. Hollis, B., Barnhardt, M., Maclean M., Duferene, A., Wadhmas, T.: Turbulent Aeroheating Measurements on a 7-deg Half- Angle Cone in a High-Enthalpy CO_2 Expansion Tunnel, Paper presented at 56th AIAA Aerospace Sciences Meeting, Florida, 8-12 January 2018
9. Tanno, H., Komuro, M., Sato, K., Itoh, K., Aeroheating measurements on capsule model with roughness in high enthalpy shock tunnel HIEST, Paper presented at the 2014 Asia-Pacific International Sympsonium on Aerospace Technology, Shangai, 24-26 Sep 2014
10. Fahy, E, Gollan, R., Buttsworth, D., Jacobs, P., Morgan, R.: Experimental and computational fluid dynamics studies of superorbital earth re-entry. Paper presented at the 46th AIAA thermophysics conference, Washington DC, 13-17 June 2016
11. de Crombrugghe, G.: On binary scaling and ground-to-flight extrapolation in high-enthalpy facilities. Dissertation, University of Queensland (2017)
12. Eichmann, T.: Radiation measurements in a simulated Mars atmosphere. Dissertation, University of Queensland (2012)

13. Gildfind, D., Morgan, R., Jacobs, P.: Expansion tubes in Australia. In Experimental methods on shock wave research, pp. 414-415. Springer, Basel (2016)

14. Hornung, H. G.: 28th Lancaster Memorial Lecture-Experimental real gas hypersonics. Aeronaut. J. **92**, 379-389 (1988)

15. de Crombrugghe, G., Gildfind, D., Zander, F., McIntyre, T., Morgan, R.: Design of Test Flows to Investigate Binary Scaling in High Enthapy CO_2-N_2 mixtures. Paper presented at the 11th Australasian Fluid Mechanics Conference, Melbourne, Australia, 8-11 December 2014

16. Anderson, J.D.: Hypersonics and high temperature gas dynamics. American Institute of Aeronautics and Astronautics, Reston, VA (2000).

17. Edquist, K.T, Dyakonov, A., Wright, M., Tang, C.: Aerothermodynamic Design of Mars Science Laboratory Heatshield. Paper presented at the 41st AIAA Thermophysics Conference, San Antonio, 22-25 June 2009

18. Hollis, B., Liechty, D., Wright, M.J., Holden, M.S., Wadhams, T.P., Maclean, M., Dyaknonov, A.: Transition Onset and Turbulent Heating Measurements for the Mars Science Laboratory Entry Vehicle. Paper presented at the 43rd AIAA Aerospace Sciences Meeting and Exhibit, Reno, 10-13 January 2005

19. Edquist, K., Hollis, B., Johnston, C., Bose, D., White, T., and Mahzari, M.: Mars Science Laboratory Heat Shield Aerothermodynamics: Design and Reconstruction. J. Spacecr. Rockets. **51**, 1106–1124 (2014)

20. Gildfind, D.E, James, C.M., Morgan, R.G.: Free piston driver performance characterisation using experimental shock speeds through helium. Shock.Waves, **25**, 169-176 (2015)

21. James, C., Gildfind, D.E., Lewis, S.W., Morgan, R., and Zander, F.: Implementation of state-to-state analytical framework for the calculation of expansion tube flow properties. Shock. Waves. **28**, 1–29 (2017)

22. Gildfind, D.E, Morgan, R.G, Jacobs, P.A, McGilvray, M.: Production of high-Mach-number scramjet flow conditions in an expansion tube. AIAA J. **52**, 162-177 (2014)

23. Mirels, H.: Shock tube test time limitation due to turbulent wall boundary layer. AIAA J. **2**, 84-93 (1964)

24. Mirels, H.: Test time in low pressure shock tubes. Phys. fluids. **6**, 1201-1214 (1963)